Theory of Brillouin scattering from corrugated surfaces

A. M. Marvin
Dipartimento di Fisica Teorica, Università di Trieste, Miramare-Grignano, I-34014 Trieste, Italy

F. Nizzoli and L. Giovannini*
Dipartimento di Fisica, Università di Ferrara, via Paradiso 12, I-44100 Ferrara, Italy
(Received 15 November 1994)

The phonon–surface-polariton (SP) interaction in addition to the phonon-phonon mixing is accounted for in order to get the Brillouin scattering cross section from an optical bigrating or from a rough surface of a metal. We limit our attention to nontransparent media, thus neglecting from the start the elasto-optic effect and linearize the ripple contribution in the extinction-theorem equations. We compare these results with the experimental data. In a silver grating the Rayleigh peak shows a "replica" in the frequency spectrum due to phonon-SP coupling. On the contrary, in a Si grating phonon-phonon mixing is responsible for the observed gaps in the second- and higher-order Brillouin zones.

I. INTRODUCTION

Surface Brillouin scattering has been largely used in the last decade to get information on the elastic and elasto-optic properties of transparent materials and is a well understood phenomenon.[1,2] The method is particularly suited to study surface dynamics of films and layered structures for metals and many semiconductors when the light penetration depth becomes small compared to the phonon wavelength, and the agreement between the theory and the experimental data is well established.[3]

Recently, Brillouin scattering experiments have been performed on controlled optical gratings rather then using flat surface samples and new structures observed in the spectral intensity of the backscattered light. Using a silver grating Robertson *et al.*[4] observed that for particular angles of scattering, the spectral intensity reveals a second Rayleigh replica at a higher phonon frequency Ω in addition to the ordinary Rayleigh peak. Moreover, using a Si sample, Dutcher *et al.*[5] observed a small splitting in the Rayleigh peak at the first Brillouin zone edge.

These features have been recognized as consequences of the presence of the grating which mixes modes of the same frequency but different parallel momentum on the surface. In the first case,[4] one has to deal with light-mode mixing:[6] the initial radiative state goes into an evanescent wave, hence, at particular angles, it can resonate with a surface polariton (SP). The surface Rayleigh mode constitutes the principal contribution to the inelastic intensity and there are essentially two scattering processes involved. One is the direct transition from the initial to the final state, which gives rise to the usual Rayleigh peak; the other involves the intermediate, virtual, and long living SP state which generates the observed Rayleigh replica.

The appearance of a Ω gap at the zone border in the Si grating[5] is instead a consequence of the standard phonon-mode mixing, i.e., the coupling of two surface waves of opposite momenta. More interesting, however, is the presence of another and even larger gap observed by Dutcher *et al.*[5] in the second Brillouin zone and whose explanation is far from being trivial. In fact, it has been recognized[7,8] that this second and larger gap originates from a mixing of the Rayleigh wave with the longitudinal bulk threshold which acts like a pseudosurface mode.

This shows that light as well as phonon modes have to be properly treated on a grating. In other words, the grating grooves couple light through phonons, which already feel the grating periodicity. We shall talk in this case of "dressed" phonons, to distinguish them from the "bare" ones and relative to a flat geometry.[9] Working with dressed phonons has been an essential ingredient in order to reproduce the observed splitting in Si.[5] On the contrary the light mixing seems to play a secondary role, and the observed intensity is nicely reproduced[7] with the direct process only (the influence of indirect processes via virtual states will be considered later in this paper).

Vice versa for the observed Rayleigh replica in silver,[4] the bare phonons are good enough, but one cannot get rid of light mixing, since the virtual SP state becomes now essential in order to explain the data.[6]

A consistent theory has to include at the same time all these effects. Its presentation is the aim of this paper. We are not limited to transparent media, since this is the case encountered in the experiments. Therefore, we neglect from the start the elasto-optic effect.

In Sec. II we derive the equations for a moving surface and solve them in the adiabatic limit generalizing previous results.[10,11] The theory is suited to treat Brillouin scattering since the characteristic surface vibrations are in the microwave region, and thus smoothly varying when compared with the light frequency ω. Consistently throughout the paper we neglect the small change in the light frequency ω over the phonon frequency Ω whenever possible, since $\Omega \ll \omega$. The connection with the T matrix of the scattering theory is made in Sec. III. The *effective vertex* equation for the dynamical corrugation is derived following the same procedure as in Ref. 10. In

 ©1995 The American Physical Society

Sec. IV we obtain cross-section formulas that are linear in the phonon displacements but valid in principle to all orders in the static corrugation. In Sec. V we solve for the surface Rayleigh mode and for the bulk continuum containing surface resonances.[7] Finally, in Secs. VI and VII, as applications of the theory, we present some numerical results for a one-dimensional (1D) grating on Ag and Si, which have been studied experimentally.

In this paper we are mainly interested in surface gratings. Equivalently to Glass, Loudon, and Maradudin[12] we are limited to calculate the modes of vibration on a periodic structure. However, the cross section as presented in Sec. IV is equally valid for a stochastic surface. In the latter case, the modes can be solved in a power series of the roughness. This is the approach used by Maradudin and Mills[13] for the Rayleigh wave, and can be easily extended to the bulk continuum. The roughness does not introduce relevant structures in the spectrum, a part from a broadening on the surface modes and a lowering of the thresholds, which are of less physical interest. We do not treat this argument here.

II. THE DYNAMICAL SURFACE PROBLEM

The problem of surface Brillouin scattering on a corrugated surface is solved in principle by imposing the appropriate boundary conditions on the electromagnetic (e.m.) field satisfying the homogeneous Maxwell equations

$$\nabla \times \mathbf{E} = -\frac{1}{c}\frac{\partial}{\partial t}\mathbf{B}, \quad \nabla \cdot \mathbf{E} = 0, \tag{2.1}$$

$$\nabla \times \mathbf{B} = \frac{1}{c}\frac{\partial}{\partial t}\mathbf{E} \tag{2.2}$$

which hold in all space but not on the surface of separation $\sigma(t)$ defined by

$$z = \xi(\mathbf{R}, t), \tag{2.3}$$

where $\mathbf{R} \equiv (x, y)$. In the medium confined in the region $z < \xi$ one has to add the constitutive equation

$$D_\alpha(\mathbf{r}, t) = \int \epsilon_{\alpha\beta}(t - t') E_\beta(\mathbf{r}, t') dt' \tag{2.4}$$

hence the wave equation follows:

$$\nabla^2_{\mathbf{r}'} E_\alpha(\mathbf{r}', t') - \frac{1}{c^2}\frac{\partial^2}{\partial t'^2}\int \epsilon_{\alpha\beta}(t' - t'') E_\beta(\mathbf{r}', t'') dt'' = 0. \tag{2.5}$$

Equation (2.4) implicitly assumes a *local* relation between D_α and E_β, neglecting spatial dispersion. Also $\epsilon_{\alpha\beta}$ appears to be translationally invariant in time which means that the elasto-optic effect, that is the influence of the phonon displacement on the dielectric constant, is disregarded from the beginning. To make the equations simpler we assume $\epsilon_{\alpha\beta}$ to be diagonal, i.e.,

$$\epsilon_{\alpha\beta}(t - t') = \delta_{\alpha\beta}\epsilon(t - t'). \tag{2.6}$$

These are the main assumptions of the paper, which make the theory presented here not suited to transparent and isotropic media. The solution is found through the (scalar) Green function equation

$$\nabla^2_{\mathbf{r}'} \mathcal{G}(\mathbf{r}, \mathbf{r}', t - t') - \frac{1}{c^2}\frac{\partial^2}{\partial t'^2}\int \epsilon(t - t'') \mathcal{G}(\mathbf{r}, \mathbf{r}', t'' - t') dt'' = \delta(\mathbf{r} - \mathbf{r}')\delta(t - t') \tag{2.7}$$

in the standard way, multiplying it on the left by $\mathbf{E}(\mathbf{r}', t')$ and Eq. (2.5) on the left by $\mathcal{G}(\mathbf{r}, \mathbf{r}', t - t')$, subtracting them, integrating on $\mathbf{r}'$ over the whole volume $V(t')$ occupied by the medium, and on time t'. Using the formal expansion

$$\mathbf{E}(\mathbf{r}, t) = \sum_\omega \mathbf{E}(\mathbf{r}, \omega) e^{-i\omega t}, \tag{2.8}$$

$$\mathcal{G}(\mathbf{r}, \mathbf{r}', t - t') = \sum_\omega \mathcal{G}(\mathbf{r}, \mathbf{r}', \omega) e^{-i\omega(t - t')}, \tag{2.9}$$

and the same for $\epsilon(t - t')$, the result is

$$\int dt' \int_{V(t')} d\mathbf{r}' \left[\mathbf{E}(\mathbf{r}', t')\nabla^2_{\mathbf{r}'}\mathcal{G}(\mathbf{r}, \mathbf{r}', t - t') - \mathcal{G}(\mathbf{r}, \mathbf{r}', t - t')\nabla^2_{\mathbf{r}'}\mathbf{E}(\mathbf{r}', t')\right]$$
$$+\frac{1}{c^2}\sum_{\omega,\omega'} e^{-i\omega t}\int dt' e^{-i(\omega' - \omega)t'}\int_{V(t')} d\mathbf{r}' \left\{\epsilon(\omega)\omega^2 - \epsilon(\omega')\omega'^2\right\}\mathbf{E}(\mathbf{r}', \omega')\mathcal{G}(\mathbf{r}, \mathbf{r}', \omega) = \mathbf{E}(\mathbf{r}, t). \tag{2.10}$$

Equation (2.10) holds if the observation point $\mathbf{r}$ is *inside* the volume V, while the right-hand side (rhs) vanishes if it is *external* to it. Note that if V does not depend on time, the second integral on the left-hand side vanishes, according to

$$\int dt' e^{-i(\omega' - \omega)t'} = \delta_{\omega,\omega'}. \tag{2.11}$$

More generally, if the surface $\sigma(t')$ delimiting the volume of integration $V(t')$ is slowly varying in time, the same integral is of the order $o(\Omega/\omega)$, Ω being here a typical phonon frequency. Neglecting corrections of order $o(\Omega/\omega)$, using the Gauss theorem, and taking the observation point $\mathbf{r}$ in vacuum, Eq. (2.10) becomes

$$\int dt' \int_{\sigma(t')} \{\mathbf{E}\partial'_n\mathcal{G} - \mathcal{G}\partial'_n\mathbf{E}\}\, dS' = 0. \tag{2.12}$$

This equation generalizes the *extinction theorem*[10,14] to

a slowly moving surface $\sigma(t')$. In it $\partial_n' = \hat{\mathbf{n}} \cdot \nabla_{\mathbf{r}'}$ where $\hat{\mathbf{n}}$ is the unit vector normal to the surface and pointing in vacuum. Again for a static surface, Eq. (2.12) contains a convolution and thus decouples in the time–Fourier-transform ω quantities. It is in the last form that a vector integral equivalent to (2.12) has been written by Jackson.[15] Using Jackson's procedure but working with the time dependent quantities, it can be easily shown that Eq. (2.12) can be equivalently transformed into

$$\int dt' \int_{\sigma(t')} \left[-\left(\hat{\mathbf{n}} \times \frac{1}{c} \frac{\partial}{\partial t'} \mathbf{B}(\mathbf{r}', t') \right) + E_n(\mathbf{r}', t') \nabla_{\mathbf{r}'} \mathcal{G}(\mathbf{r}, \mathbf{r}', t - t') + [\hat{\mathbf{n}} \times \mathbf{E}(\mathbf{r}', t')] \times \nabla_{\mathbf{r}'} \mathcal{G}(\mathbf{r}, \mathbf{r}', t - t') \right] dS' = 0. \quad (2.13)$$

The $\mathbf{E}$ and $\mathbf{B}$ quantities above are the fields on the surface taken from *inside* the medium, that is with $z \to \xi^-$. Equation (2.13) can be handled as follows: first, expressing the field quantities appearing here in terms of the field *outside* the medium, second, satisfying Eq. (2.13) with the observation point $\mathbf{r} = (\mathbf{R}, z)$ for

$$z > \max \xi(\mathbf{R}', t'), \quad (2.14)$$

that is above the grooves, and third, using the *Rayleigh hypothesis*[14] for the field expansion.

For the first point one uses the boundary conditions for the ω quantities as

$$E_n^{\text{in}}(\omega) = E_n^{\text{out}}(\omega)/\epsilon(\omega), \quad (2.15)$$

$$E_{\parallel}^{\text{in}}(\omega) = E_{\parallel}^{\text{out}}(\omega), \quad B_{\parallel}^{\text{in}}(\omega) = B_{\parallel}^{\text{out}}(\omega), \quad (2.16)$$

where "in" and "out" mean the field in the limits $z \to \xi^-$ and $z \to \xi^+$, respectively, and $\parallel$ and n are projections on the tangent plane and on the normal to it. Using the Green function representation

$$\mathcal{G}(\mathbf{r}, \mathbf{r}', \omega) = \frac{1}{L^2} \sum_{\mathbf{K}} \left(\frac{-i}{2q} \right) e^{iq|z - z'|} e^{i\mathbf{K} \cdot (\mathbf{R} - \mathbf{R}')}, \quad (2.17)$$

with

$$q \equiv q(\mathbf{K}, \omega) = \sqrt{\epsilon(\omega) \left(\frac{\omega}{c} \right)^2 - K^2}, \quad \text{Im}\, q > 0, \quad (2.18)$$

the second point allows us to drop the modulus in the exponent in (2.17).

Third, the Rayleigh hypothesis implies that for the field in vacuum, which consists of an incident wave plus a diffracted field as

$$\mathbf{E}(\mathbf{r}, \omega) = \delta_{\omega, \omega_i} \mathbf{E}_{\text{inc}}(\mathbf{r}, \omega_i) + \mathbf{E}_d(\mathbf{r}, \omega), \quad (2.19)$$

one is allowed to use an expansion

$$\mathbf{E}_d(\mathbf{r}, \omega) = \sum_{\mathbf{K}} \left[\left(\hat{\mathbf{K}} - \frac{K}{p} \hat{\mathbf{z}} \right) A_p(\mathbf{K}, \omega) + \left(\hat{\mathbf{z}} \times \hat{\mathbf{K}} \right) A_s(\mathbf{K}, \omega) \right] e^{ip z} e^{i\mathbf{K} \cdot \mathbf{R}} \quad (2.20)$$

which we suppose to be valid within the grooves up to the surface $z \to \xi^+$. Instead, the quantity $\mathbf{E}_{\text{inc}}$ in (2.19) is the incident wave containing "p" and "s" polarization

$$\mathbf{E}_{\text{inc}}(\mathbf{r}, \omega_i) = \left[\left(\hat{\mathbf{K}}_i + \frac{K_i}{p_i} \hat{\mathbf{z}} \right) A_{p,\text{inc}} + (\hat{\mathbf{z}} \times \hat{\mathbf{K}}_i) A_{s,\text{inc}} \right] e^{-ip_i z} e^{i\mathbf{K}_i \cdot \mathbf{R}}, \quad (2.21)$$

where $A_{p,\text{inc}}, A_{s,\text{inc}}$ are known coefficients.

In above the sum over ω and $\mathbf{K}$ means integrals according to

$$\sum_{\omega} \to \int \frac{d\omega}{2\pi}, \quad \sum_{\mathbf{K}} \to L^2 \int \frac{d\mathbf{K}}{(2\pi)^2} \quad (2.22)$$

with L^2 in (2.17) being the area of the sample. We use discrete indices for frequency, too, since it simplifies the notation. The continuous limit is taken at the end of the calculation. The quantities $\hat{\mathbf{K}} = \mathbf{K}/K$ and $\hat{\mathbf{z}}$ denote unit vectors, while in Eq. (2.20) we introduced

$$p \equiv p(\mathbf{K}, \omega) = \sqrt{\left(\frac{\omega}{c} \right)^2 - K^2} \quad (2.23)$$

and in Eq. (2.21) $p_i \equiv p(\mathbf{K}_i, \omega_i)$, as light momenta along the z axis in vacuum. Using the above expressions the extinction theorem Eq. (2.13) provides an equation for the unknown coefficients A_p, A_s. After some straightforward algebra one gets

$$\sum_{\omega', \mathbf{K}'} D^-(\mathbf{K}, \omega, \mathbf{K}', \omega') A(\mathbf{K}', \omega', \mathbf{K}_i, \omega_i) + D^+(\mathbf{K}, \omega, \mathbf{K}_i, \omega_i) = 0. \quad (2.24)$$

As in Ref. 10 we have introduced the 2×2 unknown matrix

$$A(\mathbf{K}, \omega, \mathbf{K}_i, \omega_i) = \begin{pmatrix} \left(\frac{\omega}{c}\right)/p\, A_p(\mathbf{K}, \omega) \\ A_s(\mathbf{K}, \omega) \end{pmatrix} \left\{ -\left[\left(\frac{\omega_i}{c} \right)/p_i A_{p,\text{inc}} \right]^{-1}, (A_{s,\text{inc}})^{-1} \right\} \quad (2.25)$$

with

$$D^-(\mathbf{K}\omega, \mathbf{K}', \omega') = \frac{1}{(q - p')} \left(e^{-i(q-p')\xi} \right)_{\mathbf{K}-\mathbf{K}', \omega-\omega'} \begin{pmatrix} (\omega/\omega')\{KK' + \hat{\mathbf{K}} \cdot \hat{\mathbf{K}}' p' q\} & -\{\frac{\omega}{c} q \hat{\mathbf{K}} \times \hat{\mathbf{K}}' \cdot \hat{\mathbf{z}}\} \\ (\omega/\omega')\{\frac{\omega}{c} p' \hat{\mathbf{K}} \times \hat{\mathbf{K}}' \cdot \hat{\mathbf{z}}\} & (\frac{\omega}{c})^2 \hat{\mathbf{K}} \cdot \hat{\mathbf{K}}' \end{pmatrix} \quad (2.26)$$

and

$$D^+(\mathbf{K},\omega,\mathbf{K}',\omega') = D^-(\mathbf{K},\omega,\mathbf{K}',\omega'\,;\, p' \to -p'). \quad (2.27)$$

The compact notation $q \equiv q(\mathbf{K},\omega), p' \equiv p(\mathbf{K}',\omega')$ is used, and the first term on the rhs in (2.26) denotes the Fourier transform in space and time defined as

$$(g)_{\mathbf{K}} = \frac{1}{L^2}\int g(\mathbf{R})e^{-i\mathbf{K}\cdot\mathbf{R}}d\mathbf{R} \quad (2.28)$$

and

$$(f)_{\omega} = \int f(t)e^{i\omega t}dt. \quad (2.29)$$

Equation (2.24) generalizes the result by Brown *et al.*[10] (their Eq. 3.1) to a slowly moving surface. Once again the Rayleigh hypothesis decouples the field in vacuum from the field in the medium. The advantage of defining the A matrix as in Eq. (2.25) is that the modulus square of its matrix elements give the scattered Poynting vector normalized to the incident one for various polarizations.

In the following we shall not distinguish, unless necessary, between ω and ω'. This allows us to put, consistently with Eq. (2.12), $\omega/\omega' \simeq 1$ in the 2×2 matrix in (2.26). Vice versa this cannot be done in the term in front of the matrix which denotes the Fourier transform in time and involving phonon frequencies

$$\Omega_n = |\omega - \omega'| \ll \omega_i. \quad (2.30)$$

III. THE VECTOR THEORY OF INELASTIC LIGHT SCATTERING

Equation (2.24) forms the basis of the vector theory of light scattering from a slowly moving surface. The zero-order reflectance can be evidenced redefining A through T as

$$\begin{aligned} A(\mathbf{K},\omega,\mathbf{K}_i,\omega_i) = {} & R(\mathbf{K},\omega,\mathbf{K}_i,\omega_i) \\ & -2ip_iG^0(\mathbf{K},\omega)T(\mathbf{K},\omega,\mathbf{K}_i,\omega_i) \\ & \times G^0(\mathbf{K}_i,\omega_i), \end{aligned} \quad (3.1)$$

where[10,11]

$$R_{\alpha\beta}(\mathbf{K},\omega,\mathbf{K}',\omega') = \delta_{\mathbf{K},\mathbf{K}'}\delta_{\omega,\omega'}\delta_{\alpha,\beta}R_{\alpha}(\mathbf{K},\omega), \quad (3.2)$$

$$R_1 = (\epsilon p - q)/(\epsilon p + q), \quad R_2 = (p - q)/(p + q) \quad (3.3)$$

are Fresnel coefficients for a smooth surface, and

$$G^0_{\alpha\beta}(\mathbf{K},\omega) = \delta_{\alpha,\beta}G^0_{\alpha}(\mathbf{K},\omega), \quad (3.4)$$

$$G^0_1 = i\epsilon/(\epsilon p + q), \quad G^0_2 = i/(p + q) \quad (3.5)$$

are zero-order Green functions for p and s polarization. Inserting Eq. (3.1) in Eq. (2.24) one has

$$\begin{aligned} \sum_{\omega',\mathbf{K}'} & D^-(\mathbf{K},\omega,\mathbf{K}'\omega')G^0(\mathbf{K}',\omega')T(\mathbf{K}',\omega',\mathbf{K}_i,\omega_i) \\ & = -\frac{1}{2p_i}\{D^+(\mathbf{K},\omega,\mathbf{K}_i,\omega_i)h^+(\mathbf{K}_i,\omega_i) \\ & \quad + D^-(\mathbf{K},\omega,\mathbf{K}_i,\omega_i)h^-(\mathbf{K}_i,\omega_i)\} \end{aligned} \quad (3.6)$$

or in compact notation

$$D^-G^0T = -\tfrac{1}{2}\left(D^+h^+ + D^-h^-\right)\mathcal{P}, \quad (3.7)$$

where $h^+ = iG^{0^{-1}}$, $h^- = iRG^{0^{-1}}$ are diagonal matrices $h^{\pm}_{\alpha\beta} = \delta_{\alpha,\beta}h^{\pm}_{\alpha}$ with

$$h^{\pm}_1(\mathbf{K},\omega) = (\epsilon p \pm q)/\epsilon, \quad h^{\pm}_2(\mathbf{K},\omega) = p \pm q. \quad (3.8)$$

We have defined for convenience the quantity $\mathcal{P}(\mathbf{K},\omega) = [1/p(\mathbf{K},\omega)]\,\mathbf{1}$ where $\mathbf{1}$ is the unit matrix. Equivalently with

$$T = V + TG^0V \quad (3.9)$$

and multiplying Eq. (3.7) on the right by $(\mathbf{1} - G^0V)$ one gets the equation for the *effective* vertex V

$$\left(D^- - D^+\right)\mathcal{P}V = i\left(D^-h^- + D^+h^+\right)\mathcal{P}. \quad (3.10)$$

Equation (3.9) resembles the T-matrix equation of the scattering theory and is related to the Green function G satisfying the equation

$$G = G^0 + G^0VG. \quad (3.11)$$

In fact, rewriting the last equation in the equivalent form $(1 - G^0V)G = G^0$, then multiplying it on the left by T and using $T(1 - G^0V) = V$, which is equivalent to Eq. (3.9), one gets the wanted relation

$$VG = TG^0. \quad (3.12)$$

In place of Eq. (3.9) and Eq. (3.11) one then has

$$T = V + VGV, \quad (3.13)$$

$$G = G^0 + G^0TG^0. \quad (3.14)$$

From the last above equation, Eq. (3.1) becomes

$$A(\mathbf{K},\omega,\mathbf{K}_i,\omega_i) = -\delta_{\mathbf{K},\mathbf{K}_i}\delta_{\omega,\omega_i}\mathbf{1} - 2ip_iG(\mathbf{K},\omega,\mathbf{K}_i,\omega_i), \quad (3.15)$$

which can be regarded as the final result.

However, for application to Brillouin scattering, one needs only expressions linear in the phonon displacements $\mathbf{u}$. This means that the V vertex can be expanded accordingly to

$$V \simeq V^{\zeta} + V^{u} + o(u^2), \quad (3.16)$$

where V^{ζ} is the elastic interaction, and for inelastic channels V^u is linear in the phonon displacement. In order to get this expansion one needs first a relation between the dynamical surface (2.3) and the static one that we shall call

$$z = \zeta(\mathbf{R}). \quad (3.17)$$

This relation is given below.

Let be $\mathbf{u}_0 \equiv (\mathbf{U}_0\,, u_{z\,0})$, the acoustic wave amplitude at the point $\mathbf{R}_0$ at the static surface and at the time t. By definition

$$\xi(\mathbf{R},t)\,|_{\mathbf{R}=\mathbf{R}_0+\mathbf{U}_0} = u_{z\,0} + \zeta(\mathbf{R}_0)\,. \tag{3.18}$$

Eliminating now the quantity $\mathbf{R}_0$ and linearizing, one gets

$$\xi(\mathbf{R},t) - \zeta(\mathbf{R}) \simeq u_\perp(\mathbf{R},t) + o(u^2) \tag{3.19}$$

with

$$u_\perp(\mathbf{R},t) = u_z(\mathbf{R},t) - \mathbf{U}(\mathbf{R},t)\cdot\nabla\zeta(\mathbf{R}). \tag{3.20}$$

The difference between the static and dynamical surfaces is just the acoustic wave amplitude projected over the surface normal $(\hat{\mathbf{z}}, -\nabla\zeta)$, a result that would be expected from the start.

Insert now (3.16) in (3.11) and get

$$G = G^\zeta + G^\zeta V^u G, \tag{3.21}$$

where

$$G^\zeta = G^0 + G^0 V^\zeta G^\zeta. \tag{3.22}$$

The easiest way to show that the two above expressions are in fact equivalent to Eq. (3.11) is to multiply Eq. (3.21) on the left by $(1 - G^0 V^\zeta)$ and use Eq. (3.22).

To order $o(\mathbf{u})$, Eq. (3.21) solves in

$$G = G^\zeta + G^\zeta V^u G^\zeta. \tag{3.23}$$

Again, linearizing Eq. (3.13) in V^u, one gets

$$T = V^u + V^\zeta G^\zeta V^u + V^u G^\zeta V^\zeta + V^\zeta G^\zeta V^u G^\zeta V^\zeta. \tag{3.24}$$

This turns out to be consistent with Eq. (3.14) again to order $o(\boldsymbol{\mu})$ writing

$$\begin{aligned} G^0 T G^0 = G = G^\zeta V^u G^\zeta = G^0(1 + V^\zeta G^\zeta)V^u \\ \times(1 + G^\zeta V^\zeta)G^0, \end{aligned} \tag{3.25}$$

where in the second and third equalities we have used (3.23) and (3.22). In Eq. (3.24) one recovers the starting equation (but with the last term missing) that two of us (A.M.M. and F.N.) have used in a previous paper [see Eq. (12) in Ref. 6].

In conclusion, we summarize the result valid for inelastic channels writing

$$\begin{aligned} G(\mathbf{K},\omega,\mathbf{K}_i,\omega_i) &= G^0(\mathbf{K})T(\mathbf{K},\mathbf{K}_i;u_{\perp\,\omega-\omega_i})G^0(\mathbf{K}_i) \\ &= \sum_{\mathbf{K}_1,\mathbf{K}_2} G^\zeta(\mathbf{K},\mathbf{K}_1)V^u(\mathbf{K}_1,\mathbf{K}_2;u_{\perp\,\omega-\omega_i}) \\ &\quad\times G^\zeta(\mathbf{K}_2,\mathbf{K}_i). \end{aligned} \tag{3.26}$$

The explicit expression of V^u and its dependence on $u_{\perp\,\omega-\omega_i}$, the Fourier transform of Eq. (3.20), will be given later.

IV. THE INELASTIC CROSS SECTION

The cross section is obtained from the z component of the Poynting vector for the e.m. field in vacuum

$$\mathbf{S}(\mathbf{r},t) = \frac{c}{4\pi}\,[\mathbf{E}(\mathbf{r},t)\times\mathbf{B}(\mathbf{r},t)]\,. \tag{4.1}$$

This quantity must be divided by the corresponding incident flux and averaged as described below. Using the expansion (2.8) for the field, we end up (before averaging) with a double sum over $\mathbf{K}$ and ω of the kind,

$$\mathbf{S} \sim \sum_{\mathbf{K},\mathbf{K}',\omega,\omega'} . \tag{4.2}$$

The average is made, first, over the surface L^2 of the sample and second, over the Bose distribution. In the first case, one uses (2.20) and the relation

$$\frac{1}{L^2}\int e^{i(\mathbf{K}-\mathbf{K}')\cdot\mathbf{R}}d\mathbf{R} = \delta_{\mathbf{K},\mathbf{K}'} \tag{4.3}$$

which reduces Eq. (4.2) to a single sum over momenta. In the same way the temperature averaging implies that the second sum over ω' disappears. The last simplification comes from the time translational invariance of the phonon operators which gives $\delta(\omega-\omega')$ on the rhs in Eq. (4.2), in analogy to the flat surface geometry.[9] Using the same nomenclature used there,[9] we write

$$\mathbf{u}(\mathbf{r},t) = \frac{1}{L\rho^{1/2}}\sum_{\mathbf{Q},n} e^{i\mathbf{Q}\cdot\mathbf{R}}\mathbf{w}^n_{\mathbf{Q}}\mathcal{A}_{\mathbf{Q},n}(t), \tag{4.4}$$

where $\mathbf{w}^n_{\mathbf{Q}} \equiv \mathbf{w}^n(z,\mathbf{R};\mathbf{Q})$ are the normal modes of vibration, and

$$\mathcal{A}_{\mathbf{Q},n}(t) = \sqrt{\frac{\hbar}{2\Omega_n}}\left(a^n_{\mathbf{Q}}e^{-i\Omega_n t} + a^{n\,\dagger}_{-\mathbf{Q}}e^{i\Omega_n t}\right) \tag{4.5}$$

the normal coordinates, with $a^\dagger$, a the standard creation and destruction phonon operators. The average over the Bose distribution gives the above mentioned invariance

$$\langle\mathcal{A}_{\mathbf{Q},n}(t)\mathcal{A}^\dagger_{\mathbf{Q}',n'}(t')\rangle = \delta_{\mathbf{Q},\mathbf{Q}'}\delta_{n,n'}\langle\mathcal{A}_{\mathbf{Q},n}(t-t')\mathcal{A}^\dagger_{\mathbf{Q},n}(0)\rangle. \tag{4.6}$$

The normal modes appearing in (4.4) are well defined for any periodic surface and not necessarily flat. Their solutions postponed in the next section are the Bloch solutions periodic in the $\mathbf{R}$ coordinate, and characterized by the quantity $\mathbf{Q}$, the parallel pseudomomentum.

As it is well known, there are two possibilities of counting those states: first, using the *restricted* zone scheme where $\mathbf{Q}$ is confined in the first Brillouin zone. In this case, the index n is also an interband in addition to an intraband and polarization index. Second, in the *extended* zone scheme, $\mathbf{Q}$ is allowed to vary freely. In this last case, $\mathbf{Q}$ fixes the band, thus n represents the remaining parameters, i.e., the energy Ω_n of the mode and its polarization j within the band. We shall use this second representation. With this choice n is the same index as it was in the flat geometry.[9] By definition the normal modes have to satisfy the orthonormality condition

$$\frac{1}{L^2}\int d\mathbf{R}\, e^{i(\mathbf{Q}-\mathbf{Q}')\cdot\mathbf{R}} \int_{z<\zeta} dz\, \mathbf{w}^n_{\mathbf{Q}}\cdot\mathbf{w}^{n'\,*}_{\mathbf{Q}'} = \delta_{\mathbf{Q},\mathbf{Q}'}\delta_{j,j'}\delta(\Omega_n-\Omega_{n'}), \quad (4.7)$$

where the modes are *bulk modes* characterized by a continuous spectrum. For surface modes the same relation applies but in this case the last Dirac δ in frequencies is missed: the surface state being fully determined by $\mathbf{Q}$ and the polarization index j alone.

At this point one has all the ingredients to calculate the cross section. To do this it is convenient to use the linearity of the problem and to calculate G in (3.15) that is V^u appearing in (3.26), taking "one mode $\mathbf{w}^n_{\mathbf{Q}}$ at a time," and summing over the modes (i.e., over n) at the end. Again, being the vertex V^u linear in $u_\perp$, it is convenient to factorize it out and redefine

$$V^u(u_{\perp\,\omega-\omega_i}) \to V^u\left([w_\perp{}^n_{\mathbf{Q}}]\right)(\mathcal{A}_{\mathbf{Q},n}(t))_{\omega-\omega_i}. \quad (4.8)$$

Here the square brackets denote that V^u is a linear functional of $w_\perp$ which, in analogy to (3.20), is defined to be the surface quantity

$$w_\perp{}^n_{\mathbf{Q}} \equiv w_\perp{}^n_{\mathbf{Q}}(\mathbf{R}) = \left\{w^n_z(z,\mathbf{R};\mathbf{Q}) - \mathbf{W}^n(z,\mathbf{R};\mathbf{Q})\cdot\nabla\zeta(\mathbf{R})\right\}_{z=\zeta}. \quad (4.9)$$

As already specified, the subscript $\omega-\omega_i$ present on both sides in (4.8) denotes the time-Fourier transform. From the above definition the rhs in (4.2) contains the product

$$\langle\mathcal{A}_{\mathbf{Q},n}(t)_{\omega-\omega_i}\mathcal{A}_{\mathbf{Q},n}(t')_{\omega'-\omega_i}\rangle = (2\pi)^2\delta(\omega'-\omega)\delta\left(\Omega_n-|\omega-\omega_i|\right)\frac{\hbar\tilde{N}(\omega-\omega_i)}{2|\omega-\omega_i|} \quad (4.10)$$

with $\tilde{N}(\Delta\omega) = |\exp(\Delta\omega/K_BT)-1|^{-1}$ and such that $\tilde{N} = N, N+1$ for anti-Stokes and Stokes processes, N being the Bose factor.

From Eq. (4.1) and using Eq. (3.15) the differential cross section becomes

$$\left(\frac{d^2\sigma}{d\Omega_f\, d\omega_f}\right)_{\alpha\leftarrow\beta} = \frac{1}{\pi^2}\left(\frac{\omega}{c}\right)^4\cos^2\theta_f\cos\theta_i\frac{\hbar\tilde{N}(\omega_f-\omega_i)}{2\rho|\omega_f-\omega_i|} \times\sum_{\mathbf{Q},n}\delta\left(|\omega_f-\omega_i|-\Omega_n\right) \times|G_{\alpha\beta}(\mathbf{K}_f,\mathbf{K}_i\,;\,[w_\perp{}^n_{\mathbf{Q}}])|^2 \quad (4.11)$$

and the Green function is found through Eqs. (3.26) and Eq. (4.8), i.e., more precisely from

$$G_{\alpha\beta}\left(\mathbf{K}_f,\,\mathbf{K}_i;\,[w_\perp{}^n_{\mathbf{Q}}]\right) = G^0_\alpha(\mathbf{K}_f)T_{\alpha\beta}\left(\mathbf{K}_f,\mathbf{K}_i,\omega;\,[w_\perp{}^n_{\mathbf{Q}}]\right)\Big|_{\Omega_n=|\omega-\omega_i|}G^0_\beta(\mathbf{K}_i) = \sum_{\gamma,\delta}\sum_{\mathbf{K}_1,\mathbf{K}_2}G^\zeta_{\alpha\gamma}\left(\mathbf{K}_f,\mathbf{K}_1\right)V^u_{\gamma\delta}\left(\mathbf{K}_1,\mathbf{K}_2,\omega\,;\,[w_\perp{}^n_{\mathbf{Q}}]\right)\Big|_{\Omega_n=|\omega-\omega_i|}G^\zeta_{\delta\beta}\left(\mathbf{K}_2,\mathbf{K}_i\right). \quad (4.12)$$

As already noted we do not distinguish ω_f, ω_i unless necessary, and name them ω. For simplicity we also drop in the last expression the ω dependence in G^ζ and G^0.

Equation (4.11) is the main result of the paper. Its derivation has been made for a periodic grating, but the same result remains valid for a stochastic surface. To this purpose one makes the replacement $|G|^2 \to \langle\!\langle|G|^2\rangle\!\rangle$, where $\langle\!\langle\ \rangle\!\rangle$ denotes roughness averaging.

Equation (4.11) is an "*exact*" result. For numerical calculations it suffices to solve the vertex V in (3.10) to lowest order in ζ. From (3.16) we get

$$V^\zeta(\mathbf{K},\mathbf{K}'\,;\,\omega) = \zeta_{\mathbf{K}-\mathbf{K}'}\hat{U}(\mathbf{K},\mathbf{K}') \quad (4.13)$$

and

$$V^u\left(\mathbf{K},\mathbf{K}',\omega\,;\,[w_\perp{}^n_{\mathbf{Q}}]\right)\Big|_{\Omega_n=|\omega-\omega'|} = \left(w_\perp{}^n_{\mathbf{Q}}\right)_{\mathbf{K}-\mathbf{K}'-\mathbf{Q}}\Big|_{\Omega_n=|\omega-\omega'|}\hat{U}(\mathbf{K},\mathbf{K}') \quad (4.14)$$

with

$$\hat{U}(\mathbf{K},\mathbf{K}') = \left(1-\frac{1}{\epsilon}\right) \times\begin{pmatrix} KK'-\hat{\mathbf{K}}\cdot\hat{\mathbf{K}}'qq'/\epsilon & -\frac{\omega}{c}q\hat{\mathbf{K}}\times\hat{\mathbf{K}}'\cdot\hat{\mathbf{z}} \\ -\frac{\omega}{c}q'\hat{\mathbf{K}}\times\hat{\mathbf{K}}'\cdot\hat{\mathbf{z}} & \epsilon\left(\frac{\omega}{c}\right)^2\hat{\mathbf{K}}\cdot\hat{\mathbf{K}}' \end{pmatrix}. \quad (4.15)$$

Neglecting terms of order $o(\zeta)$ in Eq. (4.9), the approximate constant factor $w_\perp{}^n_{\mathbf{Q}} \simeq w^n_z(z=0\,;\,\mathbf{Q})$ appears. In fact to lowest order, the $\mathbf{R}$ dependence disappears in $\mathbf{w}$, which becomes the solution for a flat geometry. To this order Eq. (4.14) reduces to

$$V^u(\mathbf{K},\mathbf{K}',\omega\,;\,[w_\perp{}^n_{\mathbf{Q}}]) \simeq \delta_{\mathbf{Q},\mathbf{K}-\mathbf{K}'}w^n_z(z=0,\,;\,\mathbf{Q})|_{\Omega_n=|\omega-\omega'|}\hat{U}(\mathbf{K},\mathbf{K}') \quad (4.16)$$

recovering Eq. (15′) of Ref. 6. For fixed $\mathbf{Q}$, the sum over n in Eq. (4.11) runs over the surface as well as the bulk modes, implying in the second case an integration, according to Eq. (4.7).

Here we have used the *extended* zone scheme. The change to the *restricted* representation would require the replacement

$$\delta_{\mathbf{Q},\mathbf{K}-\mathbf{K}'} \to \delta_{\mathbf{Q}+\mathbf{G},\mathbf{K}-\mathbf{K}'} \quad (4.17)$$

in (4.16), while the rhs in (4.11) would contain also the sum over $\mathbf{G}$. This justifies Eq. (8) that has been used in Ref. 6.

V. NORMAL MODES

In the long wavelength limit the acoustic vibrations can be treated classically. Within the medium, which

can be viewed as an elastic continuum, the acoustic wave amplitude satisfies the elastic equation

$$\rho\Omega^2 u_i(\mathbf{r}) + \frac{\partial}{\partial x^j} c_{ijhk}(\mathbf{r};\Omega)\frac{\partial}{\partial x^k} u_h(\mathbf{r};\Omega) = 0. \quad (5.1)$$

The above equation already involves time-Fourier quantities obtained by making the usual expansion

$$\mathbf{u}(\mathbf{r},t) = \sum_{\Omega} \mathbf{u}(\mathbf{r};\Omega) e^{-i\Omega t}. \quad (5.2)$$

We describe the medium confined in the semispace $z \leq \zeta$ letting

$$c_{ijhk}(\mathbf{r}) = c_{ijhk}\theta[\zeta(\mathbf{R}) - z], \quad (5.3)$$

where c_{ijhk} are the bulk elastic coefficients, and ρ is the density. With (5.3), Eq. (5.1) reduces to the two equations below. For $z < \zeta$ it becomes the ordinary bulk elastic equation,

$$\rho\Omega^2 u_i(\mathbf{r};\Omega) + c_{ijhk}\partial^2_{jk} u_h(\mathbf{r};\Omega) = 0 \quad (5.4)$$

while for $z = \zeta$ it includes the *free stress* boundary conditions at the surface

$$\hat{n}_j T_{ij}|_{z=\zeta} = 0 \quad (5.5)$$

with $\mathbf{T}$ the stress tensor

$$T_{ij} = c_{ijhk}\partial u_h/\partial x_k. \quad (5.6)$$

As usual $\hat{\mathbf{n}}$ denotes the unit vector normal to the surface and pointing in vacuum.

In analogy to the light equation (2.5), Eq. (5.4) can be solved in terms of the appropriate Green function of the elastic problem for the bulk. This approach has been followed by Glass, Loudon, and Maradudin[12] for the propagation of the surface Rayleigh wave on an isotropic 1D grating profile. Equivalently, we use here the Rayleigh method and expand the amplitude vibration as a linear combination of bulk solutions from Eq. (5.4) according to

$$\mathbf{u}(\mathbf{r};\Omega) = \sum_{\mathbf{q}^T_{(\lambda)}} C_\lambda \left(\mathbf{q}^T_{(\lambda)}\right) \mathbf{e}\left(\mathbf{q}^T_{(\lambda)}\right) e^{i\mathbf{q}^T_{(\lambda)}\cdot\mathbf{r}}, \quad (5.7)$$

where C_λ are appropriate coefficients. As will appear clear in a moment, it becomes useful to rewrite Eq. (5.7) in the equivalent form

$$\mathbf{u}(\mathbf{r};\Omega) = \sum_{\mathbf{Q}',\lambda} C^-_\lambda(\mathbf{Q}')\mathbf{e}^-_\lambda(\mathbf{Q}')e^{-iq'_\lambda z}e^{i\mathbf{Q}'\cdot\mathbf{R}} + \sum_{\mathbf{Q}',\lambda} C^+_\lambda(\mathbf{Q}')\mathbf{e}^+_\lambda(\mathbf{Q}')e^{+iq'_\lambda z}e^{i\mathbf{Q}'\cdot\mathbf{R}}. \quad (5.8)$$

The quantities appearing in Eq. (5.7) are defined below, and those in Eq. (5.8) are found by comparison.

Following Ref. 7, $\mathbf{e}(\mathbf{q}^T_{(\lambda)})$ are bulk solutions for λ polarization and total momentum

$$\mathbf{q}^T_{(\lambda)} \equiv (\mathbf{Q}, \pm q_\lambda), \quad T = +, - \quad (5.9)$$

obtained from Eq. (5.4), thus satisfying the secular equation

$$(\rho\Omega^2\delta_{ih} - c_{ijhk}q^T_{j\,(\lambda)}q^T_{k\,(\lambda)})e_h(\mathbf{q}^T_{(\lambda)}) = 0. \quad (5.10)$$

The z component of the phonon wave vector q_λ are chosen in the upper complex plane, i.e., they satisfy $0 \leq \arg q_\lambda < \pi$. In this way Eq. (5.8) separates the terms $T = -$ (first sum) from the terms $T = +$ (second sum). Complex solutions are accepted in the first sum, but the second sum is limited to those $\mathbf{Q}'$ and λ values, implying a purely real q'_λ.

In this way the first sum represents traveling waves from the surface *downward* in the bulk (for Im q_λ = 0) or exponentially decaying ones into the medium (if Im $q_\lambda > 0$). On the opposite the second term is visualized as a sum of "incident waves" traveling from the bulk *upward* to the surface. As we shall see later the latter sum contains a finite number of terms, which for fixed pseudomomentum $\mathbf{Q}$ of the mode, increases with the energy Ω. The unknowns C^-_λ are eliminated in terms of the C^+_λ by imposing the free stress boundary conditions (5.5); the coefficients C^+_λ are determined by the orthonormalization condition Eq. (4.7). It is understood that $\mathbf{e}^\pm_\lambda(\mathbf{Q})$ in Eq. (5.8) stands for $\mathbf{e}(\mathbf{q}^T_{(\lambda)})$ with $q^T_{z\,(\lambda)} = \pm q_\lambda$ and $T = +, -$.

Following Glass, Loudon, and Maradudin,[12] we shall limit for simplicity to an isotropic medium. The general extension to a cubic crystal can be done along the same lines and is rather cumbersome, but for a 1D grating along symmetry directions and orthogonal to the grating grooves.[7]

Inserting expansion (5.7) in Eq. (5.5) and solving in $\mathbf{Q}$ space one gets, after some algebra, the vector equation

$$\sum_{\mathbf{Q}'} H^-(\mathbf{Q},\mathbf{Q}')\,\mathbf{C}^-(\mathbf{Q}') + \sum_{\mathbf{Q}'} H^+(\mathbf{Q},\mathbf{Q}')\,\mathbf{C}^+(\mathbf{Q}') = 0. \quad (5.11)$$

Here $\mathbf{C}^\pm$ are vectors whose components are the coefficients $(C^\pm_\lambda, \lambda = 1,3)$ appearing in (5.8). $H^\pm$ are (3×3) matrices

$$H^\pm_{\mu\lambda}(\mathbf{Q},\mathbf{Q}') \equiv M_\mu\left(\mathbf{Q}, \mathbf{q}'^T_{(\lambda)}\right)\left(e^{\pm i\,q'_\lambda\zeta}\right)_{\mathbf{Q}-\mathbf{Q}'} \quad (\mu,\lambda = 1,3), \quad (5.12)$$

where $\mathbf{q}^T_\lambda$ is given in (5.9), and M_μ are the components of the vector

$$\mathbf{M}\left(\mathbf{Q},\mathbf{q}'^T_{(\lambda)}\right) = c_{11}\left\{\hat{\mathbf{z}} \mp \frac{\mathbf{Q}-\mathbf{Q}'}{q'_\lambda}\right\}\left(\mathbf{q}'^T_{(\lambda)}\cdot\mathbf{e}'\right) + c_{44}\left\{-\hat{\mathbf{z}}\left[\pm\frac{(\mathbf{Q}-\mathbf{Q}')\cdot\mathbf{Q}'}{q'_\lambda}e'_z + (\mathbf{Q}+\mathbf{Q}')\cdot\mathbf{E}'\right] + (2\mathbf{Q}-\mathbf{Q}')\,e'_z \pm q'_\lambda\mathbf{E}' \mp \frac{(\mathbf{Q}'\times\mathbf{E}'\cdot\hat{\mathbf{z}})}{q'_\lambda}\hat{\mathbf{z}}\times(\mathbf{Q}-\mathbf{Q}') \mp 2\frac{(\mathbf{Q}\times\mathbf{Q}'\cdot\hat{\mathbf{z}})}{q'_\lambda}\hat{\mathbf{z}}\times\mathbf{E}'\right\}. \quad (5.13)$$

To get (5.13) we have used the relation $c_{44} = (1/2)(c_{11} - c_{12})$ valid for an isotropic medium, and for brevity $\mathbf{e}' \equiv (\mathbf{E}', e'_z)$ stands for $\mathbf{e}(\mathbf{q}'^T_{(\lambda)})$.

Equation (5.12) does not define H uniquely, since the indices $\mu\,\lambda$ are not yet specified. For what concerns the index μ it is convenient to project the $\mathbf{M}$ vector (5.13) on the axis $\hat{\mathbf{z}}$, $\hat{\mathbf{Q}}$, and $\hat{\mathbf{z}} \times \hat{\mathbf{Q}}$. Instead, λ is ordered according to longitudinal and transverse polarization. Using the same notation as in Ref. 9, $q^T_{z\,(1)} = \pm q_l$, $q^T_{z\,(\lambda)} = \pm q_t$, for $\lambda = 2, 3$, while the bulk polarizations are

$$\mathbf{e}^{\pm}_{\lambda=1}(\mathbf{Q}) = \frac{c_l}{\Omega}(\mathbf{Q}, \pm q_l)\,, \quad \mathbf{e}^{\pm}_{\lambda=2}(\mathbf{Q}) = \frac{c_t}{\Omega}\left(\mp q_t\,\hat{\mathbf{Q}}, Q\right)\,,$$
$$\mathbf{e}^{\pm}_{\lambda=3}(\mathbf{Q}) = \hat{\mathbf{z}} \times \hat{\mathbf{Q}}, \tag{5.14}$$

where

$$q_{l(t)} \equiv q_{l(t)}(\mathbf{Q}) = \left[\frac{\Omega^2}{c^2_{l(t)}} - Q^2\right]^{1/2} \quad (\mathrm{Im}\, q_{l(t)} \geq 0) \tag{5.15}$$

with $c_l = \sqrt{c_{11}/\rho}$, $c_t = \sqrt{c_{44}/\rho} < c_l$ longitudinal and transverse velocities.

At this point it remains to show how to construct from Eq. (5.11) the normal modes appearing in the cross section (4.11). First, we introduce the auxiliary functions $\mathbf{u}_J(\mathbf{r}; \Omega)$ which can be obtained, setting in Eq. (5.11)

$$C^+_\lambda(\mathbf{Q}) = \delta_{\mathbf{Q},\mathbf{Q}_j}\delta_{\lambda,j'}. \tag{5.16}$$

For brevity J plays the role of a double index (j, j'). In other words the auxiliary functions contain a unique incident wave whose parallel momentum (here $\mathbf{Q}_j$) and polarization (j') is specified. Explicitly from (5.8)

$$\mathbf{u}_J(\mathbf{r}; \Omega) = \mathbf{e}^+_{j'}(\mathbf{Q}_j)\, e^{+i q_J z} e^{i \mathbf{Q}_j \cdot \mathbf{R}} + \sum_{\mathbf{Q},\lambda} C^-_\lambda(\mathbf{Q}; J)\mathbf{e}^-_\lambda(\mathbf{Q}) e^{-i q_\lambda z} e^{i\mathbf{Q}\cdot\mathbf{R}}. \tag{5.17}$$

The choice (5.16) is possible under the condition that q_J is real, and numbers the auxiliary functions in relation with bulk states. As an example consider Fig. 1 drawn for an isotropic medium. For each cross denoted by B, B', B'' in the Ω-Q plane there are three bulk states, thus three auxiliary functions according to $\mathbf{C}^+_B \sim (100)$, (010), (001), and the same for B', B''. For A, below the longitudinal threshold, there are only the two transverse solution, thus accordingly the two choices $\mathbf{C}^+_A \sim (010)$, (001). For A'' q_l, q_t are both imaginary and there is no choice, and no bulk states.

It can be verified directly that for a flat surface the auxiliary functions constructed are orthogonal to each other, so that, apart from a normalization factor, they are already normal modes. Instead, for a periodic surface, the auxiliary solutions $\mathbf{u}_I$ and $\mathbf{u}_J$ overlap if $\mathbf{Q}_j = \mathbf{Q}_i \mathrm{mod}[\mathbf{G}]$, but are otherwise orthogonal. The result seems obvious since H in (5.11) connects C for $\mathbf{Q}' = \mathbf{Q}\mathrm{mod}[\mathbf{G}]$. We then collect auxiliary solutions mod[$\mathbf{G}$] in classes and make a linear combination

$$\mathbf{u}'_I = \sum_I \Gamma_{IH}\mathbf{u}_H \tag{5.18}$$

within each class. To fix the ideas let m be the number of $\mathbf{u}_H$ in a given class, thus $\mathbf{u}'_I$ in (5.18) are the m normal modes to be determined. Imposing on them the orthonormalization condition (4.7), one gets the $\frac{1}{2}m(m+1)$ equations for the m^2 unknowns Γ_{IH} as

$$\sum_{H,K} \Gamma^*_{IH}\Gamma_{JK} Z_{HK} = \delta_{I,J}, \tag{5.19}$$

where

$$Z_{HK} = \pi\left\{\delta_{H,K}\left|\frac{dq_H}{d\Omega}\right|^{-1} + \sum_{\mathbf{Q},\lambda}\left|\frac{dq_\lambda}{d\Omega}\right|^{-1} C^{-*}_\lambda(\mathbf{Q}; H) \times C^-_\lambda(\mathbf{Q}; K)\right\} \tag{5.20}$$

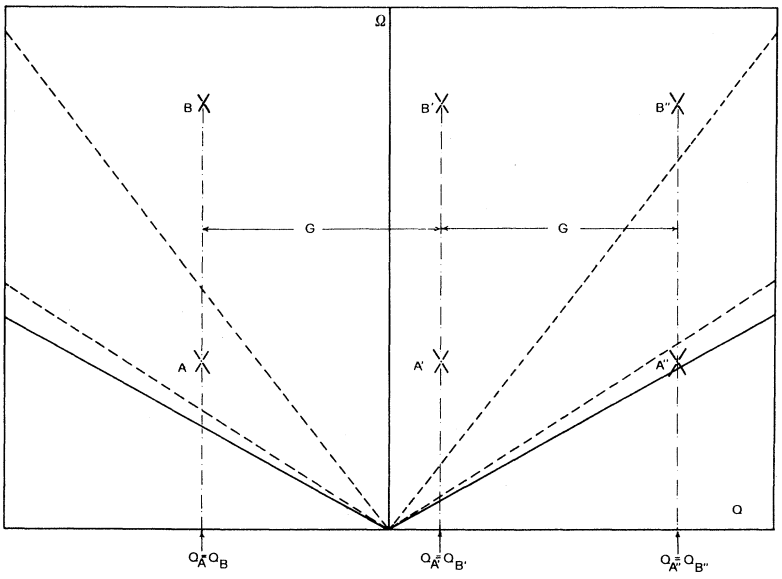

FIG. 1. Sketch of the dispersion curves for an isotropic medium. The solid lines $\Omega = c_R Q$ correspond to the Rayleigh wave on a flat geometry. The transverse threshold $\Omega = c_t Q$ delimits (from above) the continuum states. Those are two or three times degenerate according to whether they fall below or above, respectively, the longitudinal threshold $\Omega = c_l Q$.

and the last sum on the rhs is limited to the m channels where q_λ is real. The solutions can be found using the Schwartz orthogonalization procedure numbering the $\mathbf{u}_I$ solutions as $\mathbf{u}_1, \mathbf{u}_2, \ldots, \mathbf{u}_m$, then imposing $\Gamma_{rs} = 0$ for $r < s$. It can be immediately verified that the cross section Eq. (4.11), as it has to, is independent of the particular choice adopted.

To make life simple consider as an example a 1D grating, and with the grating grooves orthogonal to the propagation direction. This is an instructive case since a more general situation does not add new physics. Consider again states denoted by B, B', B'' in Fig. 1 whose wave vectors satisfy the condition $Q_{B'}, Q_{B''} = Q_B \bmod[G]$, hence belonging to the same class. There are $m = 9$ auxiliary solutions in this class. Equation (5.12) shows in addition that the transverse polarization along the grating grooves decouples from the other two. This gives two systems of separate equations: one with three and the other with six coupled equations respectively in (5.19). For A, A', A'' states, one obtains instead two and three coupled equations. This example shows that for $\mathbf{Q}(\mathrm{mod}[\mathbf{G}])$ fixed, the number of solutions m to be orthogonalized increases rapidly as the energy Ω increases. This is, of course, a general result.

To conclude this section it remains to be shown how to construct in practice the auxiliary solutions. We put the question in the following terms: how to select among infinite terms present in the first sum in Eq. (5.11), those for which $C^-_\lambda(\mathbf{Q}')$ are large?

Without restriction this can be easily visualized in 1D considering again the states in Fig. 1. For the auxiliary solution corresponding to A, one certainly has to include in addition to the diagonal contribution $Q' = Q \equiv Q_{A'}$ both the $Q' = Q + G = Q_{A''}$ and the $Q' = Q - G = Q_A$ terms. The former is closed to the Rayleigh wave (RW) existing in the flat geometry, while the latter resembles the longitudinal resonance (LR).[7,9] Accordingly, one solves for the unknowns $\mathbf{C}^-(Q_A), \mathbf{C}^-(Q_{A'}), \mathbf{C}^-(Q_{A''})$ using again Eq. (5.11) but now with $Q = Q_A$ and $Q = Q_{A''}$, then follows Ref. 7. In the same way one proceeds to build up the (two transverse) auxiliary solutions denoted by A. Here the coupling with the RW (A'') is dominant, while the inclusion of the term $Q' = Q_{A'}$ in the sum in (5.11) plays a little role and can be omitted in the first approximation. Those solutions are finally orthogonalized as in Eq. (5.18). This is an illustrative example and shows how the RW, well defined for a flat geometry, survives (in general) on a periodic surface, through the presence of the term $C^-_\lambda(Q_{A''}) \gg 1$ in the normal modes of the continuum spectrum. In other words, the Rayleigh solution becomes (in general) a "leaky" mode[16] damped by the bulk solution via the grating, and is *not* a mode of the system. Using a graphical construction in Fig. 1 one can be easily convinced that at very low frequencies, i.e., for $\Omega < \left(\frac{1}{c_R} + \frac{1}{c_t}\right)^{-1} G$, the RW still exists and remains undamped. For larger frequencies instead a damping is present. The quantity c_R is the RW velocity on a flat surface as indicated in Fig. 1.

Equivalently we can express this result as follows. Setting in Eq. (5.11) all coefficients $\mathbf{C}^+(\tilde{\mathbf{Q}}) = 0$, a real solution for Ω exists only in the low-frequency interval indicated above. For higher values a solution of the boundary conditions (5.11) for real Q exists only for complex frequencies. Vice versa starting from a real Ω, one gets solutions for Q complex. One finds in this way the damping and the mean free path of the RW on a periodic surface.[12]

Since we are interested in the cross section Eq. (4.11) we shall consider only modes for real frequencies, and in particular pay attention on the Ω gaps they generate at their crossing. Thus for $Q = \pm\frac{G}{2}$ at the first Brillouin zone (BZ) border the two (undamped) RW split and give rise to a well-known Ω gap. Less trivially a gap is present when the RW couples with the LR at $\Omega = \left(\frac{1}{c_R} + \frac{1}{c_l}\right)^{-1} G$, the last acting to all effects as a pseudosurface mode.[7] Both resonances have been seen on a Si(001) grating for an exchanged parallel momentum $\mathbf{K}_f - \mathbf{K}_i$ in the second[5] and third[16] BZ. Applications of these concepts to the realistic case of a 1D Si grating is presented in Sec. VII.

VI. NUMERICAL RESULTS FOR A SILVER GRATING

The cross section Eq. (4.11) is an exact result and can be simplified according to the problem one has in mind. As stated in the Introduction we shall consider two cases. The first is a silver grating[4] when the interaction with the SP plays an essential role. The second is a Si grating where indirect processes are less important, but in some particular circumstances appreciable.

As in a previous paper[6] we start from Eq. (4.12) and solve the T matrix in the hypothesis that the diagonal elements of G^ζ, namely $G^\zeta(\mathbf{K}, \mathbf{K})$, dominate. The easiest way to solve them is to start iterating Eq. (3.22) once, thus using its equivalent $G^\zeta = G^0 + G^0 V^\zeta G^0 + G^0 V^\zeta G^0 V^\zeta G^\zeta$. Neglecting here the second term on the rhs involving only off-diagonal contributions, we get

$$G^\zeta_{\alpha\beta}(\mathbf{K}, \mathbf{K}) = \delta_{\alpha,\beta} G^\zeta_\alpha(\mathbf{K}) \quad (\alpha, \beta = 1, 2), \tag{6.1}$$

where

$$G^{\zeta\,-1}_\alpha(\mathbf{K}) = G^{0\,-1}_\alpha(\mathbf{K}) - \sum_{\mathbf{K}'\beta} V^\zeta_{\alpha\beta}(\mathbf{K}, \mathbf{K}') G^0_\beta(\mathbf{K}') \times V^\zeta_{\beta\alpha}(\mathbf{K}', \mathbf{K}). \tag{6.2}$$

First of all we use Eq. (6.2) to reproduce the Rayleigh replica (RR) observed on silver gratings. As specified in Ref. 4, the scattering plane is parallel to the grating grooves, and the exit angle is chosen so that

$$|\mathbf{K}_f \pm \mathbf{G}| = K_{\mathrm{SP}} \tag{6.3}$$

with K_{SP} the SP momentum, solution of $\mathrm{Re}(G_1^{\zeta\,-1}) = 0$.

In the experiment $\theta_i \neq \theta_f$, that is $|\mathbf{K}_i \pm \mathbf{G}| \neq K_{\mathrm{SP}}$, showing that between the two terms on the rhs in Eq. (3.24) contributing to the RR peak (second and third), one can retain the second only (resonant) and disregard the third (nonresonant). Again, the first term in (3.24) is the direct transition contributing to the Rayleigh

peak present on a flat surface, while the fourth term represents a grating correction to it.

We simplify remarkably the calculation using for the vertex V^u the approximate expression Eq. (4.16), and accordingly the "bare" phonon modes relative to a flat geometry. This is justified by the following argument.

We note from Fig. 4 in Ref. 4 that the two peaks at $\simeq 3.8$ GHz and $\simeq 4.4$ GHz have about the same experimental width $\Gamma_e \simeq 0.6$ GHz. Now the first is a contribution of a discrete state, namely the "true" Rayleigh mode, still existing on a grating geometry. This surface mode would exibit in the unconvoluted cross section Eq. (4.11) a Dirac δ at Ω_R. On the opposite the second peak (Ω_{RR}) appears in the continuous part of the spectrum and corresponds to the RR leaky mode. If we call Γ_ζ its intrinsic linewidth induced by the corrugation ζ, the experiment shows that $\Gamma_\zeta \ll \Gamma_e$. This suggests that the mode mixing induced by the grating corrugation becomes irrelevant once averaging the theoretical cross section over the experimental window, and justifies the starting hypothesis.

In Fig. 2 we plot the height ratio of the two peaks as a function of the grating amplitude ζ_G. Note that in this figure the final angle θ_f is not fixed but determined according to Eq. (6.3) in order to pickup the maximum of the RR. One finds numerically for K_{SP} a small quadratic dependence $K_{SP} \simeq K^0_{SP} + \alpha\zeta_G^2$ with $\alpha \sim 1.7 \times 10^{-9}$ Å^{-3}. We have used in the calculation for the silver grating a dielectric constant $\epsilon = -10.5 + 0.3i$,[17] referred to a wavelength of the incident p polarized light $\lambda = 5145$ Å, a Rayleigh velocity $c_R = 1658.4$ m/s,[18] a grating periodicity $\Lambda = 7200$ Å, a corrugation $\zeta_G = 50$ Å, and an incidence angle $\theta_i = 23.7°$. The last parameter is not reported in Ref. 4, so that we have chosen that value in order to roughly reproduce the mean positions of the two peaks of Fig. 4 of Ref. 4. Therefore, the agreement with the data can be only qualitative.

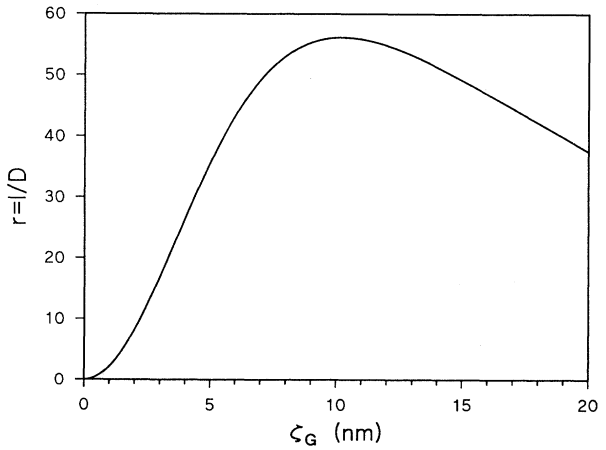

FIG. 2. Ratio of the maximum scattering intensity of the Rayleigh-replica peak (RR) over standard Rayleigh (R) for a Ag sinusoidal grating vs the corrugation strength. The incident angle is $\theta_i = 23.7°$, while θ_f is determined by the resonant condition (6.3); the geometry and other parameters are specified in the text.

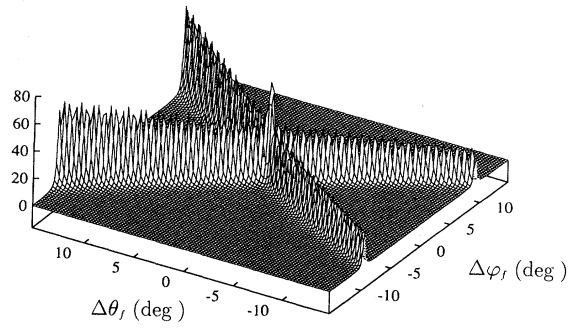

FIG. 3. The RR scattering intensity around the final angles $\theta_f = 50.8°$, and $\phi_f = 0°$. The corrugation is $\zeta_G = 50$ Å. Other parameters are given in the text.

Apparently, the large height ratio shown in Fig. 2 is in contrast with the value $r \sim 1$ one gets from the experiment. However, one has to be reminded that the acceptance angle used in the experiment is actually rather large, and the measured spectra represent the integral of the cross section over the intervals $\Delta\theta_f$ and $\Delta\phi_f$, centered, respectively, on θ_f^0 (scattering angle measured in the incident plane) and ϕ_f^0 (angle between the incidence and scattering planes). The dependence of the cross section of the RR on θ_f and ϕ_f, calculated around $\theta_f^0 = 50.8°$ and $\phi_f^0 = 0°$, is shown in Fig. 3. The intensity due to the direct Rayleigh is not shown, since within the same interval, it is a smoothly varying function. Integrating the cross sections over $\Delta\theta_f$, $\Delta\phi_f = 20°$, which correspond to commonly used collecting angles, we get a ratio $r = 0.94$, which restores the agreement with the experimental data.

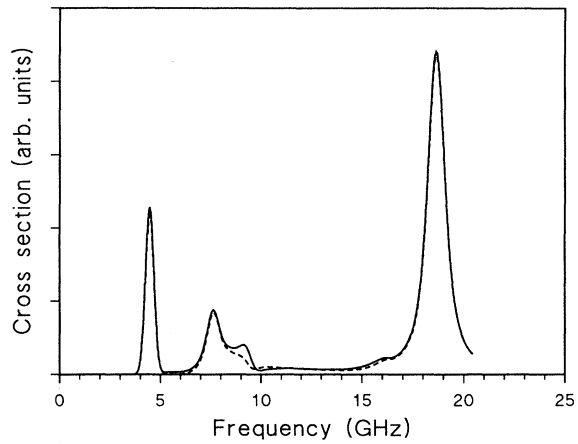

FIG. 4. The Si(001) grating intensity (backscattering) with the exchanged momentum $Q_\parallel$ in the third BZ and before the $+G$ LR and the $+2G$ leaky Rayleigh wave crossing. The grating is defined by $\zeta_G = 125$ Å, and $\zeta_{2G} = 40$ Å. The first peak is due to a discrete $+G$ Rayleigh contribution; the last is the standard Rayleigh peak of the flat surface. In between, with increasing frequency, there are the $+G$ LR and the $+2G$ leaky Rayleigh mode.

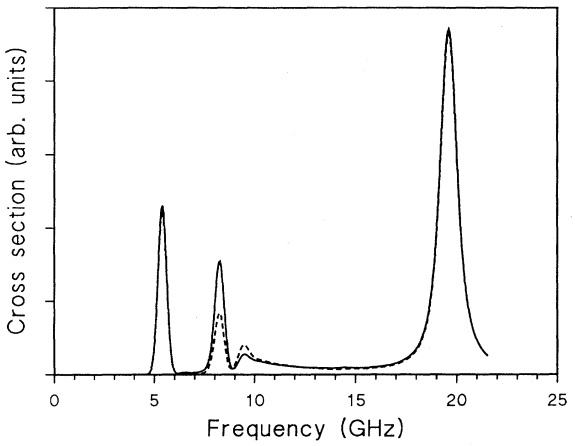

FIG. 5. As in Fig. 4, but with $Q_{\|}$ beyond the crossing between the $+G$ LR and the $+2G$ leaky Rayleigh modes. Here the second peak is the $+2G$ leaky Rayleigh mode, while the third is the $+G$ LR: these two modes are reversed, with respect to the situation shown in Fig. 4.

VII. RESULTS FOR A SILICON GRATING

As a further application of the theory we consider here a grating on the Si(001) surface, with grating wave vector **G** along [100], and the incidence plane parallel to the same direction, i.e., orthogonal to the grating grooves. In this case one must calculate the acoustic modes taking into account the grating corrugation.[7] Therefore, for the vertex V^u we use the correct Eq. (4.14) in place of Eq. (4.16) used for Ag. Our aim is to show that, in addition to the first term on the rhs of Eq. (3.24) which is certainly dominant, the other terms play an appreciable role. The exchanged momentum $Q_{\|} = K_f - K_i$ is in the third BZ; the other parameters of the calculation are defined in Ref. 16.

Figure 4 shows the spectral intensity for a wave vector that lies before the crossing of the $+G$ LR with the $+2G$ leaky Rayleigh mode.[16] The solid line is the result of the calculation reported in Fig. 1(b) of Ref. 16 and includes all the terms on the rhs of Eq. (3.24). On the contrary, the dashed line corresponds to the contribution of the first term only. The main difference is in the $+2G$ Rayleigh peak ($\sim$ 9 GHz) which is essentially due to the indirect terms. The presence of this peak was actually related[16] to the existence of a second Fourier component in the grating corrugation. In fact, by taking $\zeta_{2G} = 0$, the $+2G$ Rayleigh resonance is marked by a deep, and this happens for all reasonable values of ζ_G one uses in order to fit the remaining part of the spectrum. Our present result shows that without the inclusion of indirect terms, the agreement with the experiment can be never achieved.

As a second example we consider in Fig. 5 the same situation but for a wave vector beyond the crossing of the $+G$ LR with $+2G$ leaky Rayleigh mode. This is a calculated result and there are no experimental data for comparison. Indirect terms contribute again, as before, by $\sim$ 50%, for what concerns the second and third peaks. However, while for the $+2G$ Rayleigh mode (second peak) they add constructively to the direct contribution, for the $+G$ LR (third peak), the effect of the indirect term is to lower the intensity of the direct one (dashed line). In conclusion, for a quantitative comparison with the data, the indirect contributions in T in Eq. (3.24) cannot be neglected *a priori*.

ACKNOWLEDGMENTS

The authors gratefully acknowledge financial support from the Ministero Università e Ricerca Scientifica e Tecnologica. The research by one of us (L.G.) was supported by the Consorzio Interuniversitario Nazionale Fisica della Materia.

* Present address: Istituto di Acustica O. M. Corbino, Consiglio Nazionale delle Ricerche, Via Cassia 1216, I-00189 Roma, Italy.

[1] For a recent review article on the subject see F. Nizzoli and J.R. Sandercock, in *Dynamical Properties of Solids*, edited by G.K. Horton and A.A. Maradudin (North-Holland, Amsterdam, 1990), Vol. 6, p. 281.

[2] J.R. Sandercock, in *Light Scattering in Solids III,* edited by M. Cardona and G. Guntherodt (Springer-Verlag, Berlin, 1982), p. 173

[3] V. Bortolani, A.M. Marvin, F. Nizzoli, and G. Santoro, J. Phys. C **16**, 1757 (1983).

[4] W.M. Robertson, M. Grimsditch, A.L. Moretti, R.G. Kaufman, G.R. Hulse, E. Fullerton, and I.K. Schuller, Phys. Rev. B **41**, 4986 (1990).

[5] J.R. Dutcher, S. Lee, B. Hillebrands, G.J. McLaughlin, B.G. Nickel, and G.I. Stegeman, Phys. Rev. Lett. **68**, 2464 (1992).

[6] A.M. Marvin and F. Nizzoli, Phys. Rev. B **45**, 12160 (1992).

[7] L. Giovannini, F. Nizzoli, and A.M. Marvin, Phys. Rev. Lett. **69**, 1572 (1992).

[8] L. Giovannini, F. Nizzoli, and A.M. Marvin, Mod. Phys. Lett. B **7**, 291 (1993).

[9] A.M. Marvin, V. Bortolani, and F. Nizzoli, J. Phys. C **13**, 299 (1980).

[10] G.C. Brown, V. Celli, M. Haller, and A.M. Marvin, Surf. Sci. **136**, 381 (1984).

[11] G.C. Brown, V. Celli, M. Haller, A.A. Maradudin, and A.M. Marvin, Phys. Rev. B **31**, 4993 (1985).

[12] N.E. Glass, R. Loudon, and A.A. Maradudin, Phys. Rev. B **24**, 6843 (1981).

[13] A.A. Maradudin and D.L. Mills, Ann. Phys. (N.Y.) **100**, 262 (1976).

[14] F. Toigo, A.M. Marvin, V. Celli, and N.R. Hill, Phys. Rev. B **15**, 5618 (1977).

[15] *Classical Electrodynamics*, edited by J.D. Jackson (Wiley and Sons, Inc., New York, 1963), Sec. 9.6, p. 283.
[16] S. Lee, L. Giovannini, J.R. Dutcher, F. Nizzoli, G.I. Stegeman, A.M. Marvin, Z. Wang, J.D. Ross, A. Amoddeo, and L.S. Caputi, Phys. Rev. B **49**, 2273 (1994).
[17] P.W. Johnson and R.W. Christy, Phys. Rev. B **6**, 4370 (1972).
[18] *Microwave Acoustics Handbook*, edited by A.J. Slobodnik, Jr., E.D. Conway, and R.T. Delmonico, Surface Wave Velocities Vol. 1A (Air Force Cambridge Laboratories, Hanscom AFB, MA, 1973).